HHS Public Access

Author manuscript

Reprod Toxicol. Author manuscript; available in PMC 2017 October 01.

Published in final edited form as:

Reprod Toxicol. 2016 October ; 65: 425–435. doi:10.1016/j.reprotox.2016.05.008.

DEVELOPMENTAL CIGARETTE SMOKE EXPOSURE II: KIDNEY PROTEOME PROFILE ALTERATIONS IN 6 MONTH OLD ADULT OFFSPRING

Rachel E. Neal[a,c,d], **Rekha Jagadapillai**[b], **Jing Chen**[a], **Cynthia L. Webb**[b,c], **Kendall Stocke**[a], **Cailtin Gambrell**[a], **Robert M. Greene**[b,c], and **M. Michele Pisano**[b,c]

[a]Department of Environmental and Occupational Health Sciences, School of Public Health and Information Sciences, University of Louisville, Louisville, KY

[b]Department of Molecular, Cellular, and Craniofacial Biology, ULSD, University of Louisville, Louisville, KY

[c]Birth Defects Center, University of Louisville, Louisville, KY

Abstract

Cigarette smoke exposure (CSE) during gestation and early development suppresses the growth trajectory in offspring. In prior studies utilizing a mouse model of 'active' developmental CSE (GD1-PD21), low birth weight induced by CSE persisted throughout the neonatal period and was present at the cessation of exposure at weaning with proportionally smaller kidney mass that was accompanied by impairment of carbohydrate metabolism. In the present study, littermates of those characterized in the prior study were maintained until 6 months of age at which time the impact of developmental CSE on the abundance of proteins associated with cellular metabolism in the kidney was examined. Kidney protein abundances were examined by 2D-SDS-PAGE based proteome profiling with statistical analysis by Partial Least Squares-Discriminant Analysis. Key findings of this study include a persistence of impact of developmental CSE past the original exposure period on the nucleic acid and carbohydrate metabolism networks and oxidant scavenging pathways.

Keywords

developmental cigarette smoke exposure; CSE; proteome; kidney; mouse; inhalation; tobacco

1. INTRODUCTION

Cigarette smoke is a complex mixture composed of the addictive stimulant nicotine as well as toxic gases such as carbon monoxide, pesticides, metals, and highly reactive small

[d]Corresponding Author: rachel.neal@louisville.edu; 485 E. Gray Street, Louisville, KY 40292.

molecules such as acrolein [1–10]. 'Active' cigarette smoke consumption in adults impairs kidney function with an impact on hypertension, diabetes, and cardiovascular disease [11–15]. Despite extensive public health campaigns including product warning labels, nearly one-fifth of US women continue to smoke cigarettes during pregnancy [16–22]. Exposure of the fetus to toxic cigarette smoke results in an attendant increase in the risk of miscarriage, stillbirth, fetal intrauterine growth retardation, and low birth weight with an increased risk of ear infections, respiratory diseases, allergy/atopy, deficit/hyperactivity disorders, aggressiveness, neurocognitive delays and decreased cardiovascular health during early childhood [23–25]. At maturity, adults exposed to developmental cigarette smoke are at an increased risk of metabolic syndrome, cardiovascular disease and obesity [4, 26–29].

Similarly, in animal models, developmental cigarette smoke exposure (CSE) induces cardiovascular disease, hypertension, and a predisposition to obesity with a high fat diet challenge [30–33]. The putative link between developmental CSE and adult onset hypertension and cardiovascular disease may be attributed in part to a mild structural dysmorphology and proportionally smaller kidney size, which when coupled to obesity results in nephron hyperfiltration [34–37]. Obesity related glomerulopathy is exacerbated by reductions in nephron mass which together with obesity-induced changes in renal hemodynamics synergistically contributes to the development of glomerulopathy [38, 39]

It has been proposed that underlying metabolic dysfunction contributes to the propensity for adult onset disease in offspring developmentally exposed to cigarette smoke [30, 33, 40–43]. In our prior study of the impact of developmental CSE on kidney proteome profiles at weaning in a murine model of 'active' exposure that spanned gestation day 1 through postnatal day 21, we identified several metabolic pathways including glucose metabolism that were altered at a time point immediately after the cessation of exposure [41]. Parallel reports on the impact of this exposure paradigm on the liver and hippocampus proteomes, in the same offspring also at weaning, again identified impairment of glucose and small molecule metabolic pathways [44, 45] The study of the long term impact of developmental cigarette smoke exposure is herein presented as three manuscripts each detailing tissue-specific toxicity (liver, kidney, hippocampus [46–48]) of systemic exposure while a fourth manuscript detailing behavioral abnormalities in these identical offspring was previously presented [49]. The present manuscript examines whether the impact of developmental CSE on the kidney proteome, specifically on the expression of metabolic proteins, persists past the withdrawal of exposure and into maturity. In future studies, we will examine the impact of dietary challenge following developmental cigarette smoke exposure on tissue-specific metabolic function.

2. MATERIALS AND METHODS

2.1. Animal Exposure

Detailed descriptions of the experimental methodology can be found within the lead manuscript (liver proteome profiles [47]) for the present series of reports of sustained toxicity of developmental exposure to cigarette smoke. An abbreviated methodology section follows.

Adult C57B/6J mice were purchased from Jackson Labs (Bar Harbor, ME). Animals were housed and maintained (12 hour light/dark cycle; Purina LabDiet 5015) at the University of Louisville Research Resources Center. Female mice were age-matched at the outset of the study and timed pregnancies were obtained by overnight mating of a single mature male with two nulliparous females. The presence of a vaginal plug was considered evidence of mating and the time designated as gestational day 1 (GD1). Pregnant mice were weighed and randomly assigned to either the Sham-exposure (Sham n=9) or Cigarette Smoke Exposure (CSE; n=9) groups. Animals were exposed from GD1 throughout the entirety of gestation, and following parturition were exposed with offspring until PD21.

Cigarette smoke was generated from Philip Morris Marlboro Red brand cigarettes^{TM} (Philip Morris; Richmond, VA; 15mg of tar/cigarette; 1.1mg nicotine/cigarette; additives), selected since it represents the most popular brand of cigarettes consumed among 18-25 year olds - the age group containing the majority of maternal smokers [50–53]. Cigarettes were smoked using the standard Federal Trade Commission method: a two second, 35 cm^3 puff, once a minute for a total of 9 min [54]. For quality control purposes, dual exposure chambers (one receiving cigarette smoke and one receiving ambient air) were characterized twice during each daily exposure session for: total suspended particulates (TSP), temperature, carbon monoxide levels, and humidity.

At cessation of exposure on PD21, offspring were either euthanized for tissue collections or maintained into maturity for behavioral phenotyping at the Cincinnati Children's Research Foundation Animal Behavioral Core [49]. At approximately 6 months of age, male offspring were euthanized by CO2 asphyxiation followed by cervical dislocation [49]. Blood was collected and tissues excised, rinsed in saline, and frozen at -80^0C until analysis. Individual kidney wet weights collected from randomly selected single male offspring representing individual litters in each group (n=9 for Sham and n=8 for CSE - note one kidney weight from CSE cohort is unavailable) were averaged and reported in Figure 1.

2.2. 2D-SDS-PAGE

The upper section of a single right kidney (~0.15 g) from 9 offspring per group, each offspring representing an individual litter, was homogenized in 7M urea, 2M thiourea, and 40mM dithiothreitol (DTT). 400 μg of protein (Bradford assay; Bradford 1976) was separated by isoelectric focusing followed by SDS-PAGE on 12% gels at 65 V for 18 hours with cooling. Gels were stained for 3 days in Colloidal Coomassie Blue G-250 solution followed by water washes until a clear background was attained.

2.3. Image Analysis

Densitometric analysis of gel images (transmission scanning with Epson Expression 10000XL; 16-bit grayscale) was performed with Progenesis SameSpots software (Nonlinear Dynamics; New Castle-on-Tyne, UK). Spot patterns were aligned with manual (~20 per gel representing 4 zones) and automatic seeds (~150 per gel). Protein spots were detected automatically. For each protein spot, intensity was measured, background subtracted, and spot pixel density normalized against total pixel density of all spots on each individual gel. Spots with less than or equal to an average normalized pixel depth of 4000 were designated

as noise and not included in the analysis. The averaged normalized spot abundances for each spot on gels from the CSE group were compared to the averaged normalized aligned spot from gels of the Sham group.

2.4. Statistical Analysis

Analysis of Variance (ANOVA, two way, $p<0.05$ as significant) and a series of Partial Least Squares-Discriminant Analysis (PLS-DA) models were utilized to determine the protein spots which differed in intensity and described the differences between the groups. Multiple PLS-DA models were constructed utilizing Variable Importance in Projection (VIP)-ranked protein spots of interest with recursive feature elimination identifying protein spots with VIP≥1.75 as important in defining the separation between groups. All protein spots included in further analysis were significantly different between groups based on ANOVA ($p<0.05$).

2.5. Identification of Protein Spots

Protein spots were excised and destained then dehydrated in acetonitrile (ACN), dried, rehydrated with 10 ng/μl trypsin suspended in 40mM NH_4HCO_3, and digested at room temperature overnight. The mass to charge ratio of peptides was determined by LTQ-MS/MS with collision induced dissociation for structural feature identification. Peptide identification was performed with the Mascot (Matrix Sciences v 2.2.2) search algorithm utilizing the NCBInr (with decoy) database (updated Jan 4, 2011). Search parameters included: mammalian class; minimum of two peptide sequence hits with individual MOWSE (MOlecular Weight SEarch) probability scores greater than 45, up to 2 missed cleavages, variable carbamidomethyl C modification, enzyme trypsin/P, and peptide charge of 1^+, 2^+, or 3^+ permitted. A total MOWSE protein probability score greater than 60 was considered acceptable [55].

2.6. Ingenuity® Pathway Analysis (IPA)

Proteins of interest as determined by PLS-DA modeling and VIP ranking were loaded into the Ingenuity® Pathway Analysis search algorithm to determine metabolic pathways impacted (Ingenuity Systems, 2016). Proteins that represented the predominant contribution to the spot intensity, as determined by a minimum of 200% of the MOWSE score of the next ranked protein identified, were included. Networks of interactions between the proteins and biological pathways were generated with sub-categorization by increased or decreased abundance. For the canonical pathways analysis, the following settings were employed: Benjamin-Hochberg p-value greater than or equal to 1.5, a threshold of 0.5 z-score, and a Benjamin-Hochberg Multiple Testing Correction p-value utilized for scoring. In the associated figure (Figure 5), solid lines indicated a direct interaction while dotted lines indicate an indirect interaction. Geometric shapes identify classes of proteins: phosphatases (triangle), kinases (inverted triangle), enzymes (vertical diamond), transcription regulators (horizontal ellipse), transporters (trapezoid), and other important molecules (circles).

2.7. Western Blot

Twenty-five μg of total kidney protein homogenates were mixed 1:1 with Laemmli buffer (0.25M Tris pH 6.8, glycerol, 10% SDS, bromophenol blue trace) then heated at 70° C for

10 minutes and separated by 10% PAGE for 2 hours at a 100V in Tris-glycine run buffer (0.025 M Tris Base, 0.192 M glycine, 0.1% SDS). Electrophoretic transfer to PVDF membrane was followed by blocking and incubated overnight at 4°C with primary antibody diluted 1:500 in non-fat dry milk (SIRT1, sc-19857; PEPCK, sc-271029; PGC1α, sc-13067; Santa Cruz Biotechnology, Dallas, TX). Blots were incubated with secondary antibody complexed to horseradish peroxidase (1:1000, Santa Cruz Biotechnology, Dallas, TX) diluted in non-fat dry milk at room temperature for 1 hour. The reaction to chemiluminescence substrate was visualized then the blots were stripped and incubated with β-actin primary antibody (1:1000 dilution; sc-81173, Santa Cruz Biotechnology, Dallas TX) followed by secondary antibody incubation and visualization as described above [56].

2.8. Glutathione-S-Transferase (GST) and Glutathione Reductase (GR) Assay

Liver GST activity was measured as an indicator of detoxification activity [57]. The total GST activity of the liver was measured using the enzyme driven conjugation of 1-chloro-2, 4-dinitrobenzene (CDNB) to reduced glutathione (absorbance read at 340 nm each minute for 15 minutes; Cayman Chemical Company). The absorbance per minute was divided by amount of protein (mg) to determine the specific activity for each sample [58]. Glutathione reductase activity was measured spectrophotometrically by mixing an aliquot of tissue homogenate with GSSG and measuring the GST enzyme driven conjugation to 1-chloro-2,4-dinitrobenzene (CDNB) to reduced glutathione (absorbance read at 340 nm each minute for 15 minutes; Cayman Chemical Company) [59].

3. RESULTS

3.1. Exposure Conditions and Offspring Weights

Mean CO and TSP levels in the cigarette smoke exposure chamber were 138 ± 19.8 ppm and 25.4 ± 6.5 mg/m^3, respectively with measures in the Sham group found to be less than the limit of detection for each assay [44]. Cotinine, a metabolite of nicotine, was used as a measure of CSE dose. Cotinine levels were greater than 50ng/mL in the CSE group indicating an 'active' exposure model with Sham exposure cotinine levels below the detection limit of 4 ng/mL. Low birth weight was evident in the CSE offspring (~15% decrease relative to) [44] with persistence of decrements in weight throughout weaning and into maturity (maintenance on Purina 5015 diet) [49]. As shown in Figure 1, decreased individual averaged kidney wet weights in the CSE offspring (~10% reduction, p=0.04) were evident at maturity. This reduction in kidney tissue weight in the CSE group was proportional to the reduction in animal weight measured at the time of cognitive and behavioral assessment and therefore likely reflects a generalized proportional decrease in organism weight rather than kidney specific reductions in mass [49].

3.2. Kidney Proteome Profiles

As shown in Figure 2, 2D-SDS-PAGE gels of kidney proteins from Sham and CSE mice were similar in total pixel density (Sham, 683905790 ± 29812764; CSE, 647331403 ± 34439370; p>0.05) at 6 months of age (~5 months since cessation of exposure to cigarette smoke) indicating that the variances in individual protein spot abundance were the relevant outcome rather than an over- or under-expression of total protein within the kidney of CSE

offspring. The proteins on the gels spanned an isoelectric focusing range of pH 3 to 10, with the acidic proteins on the left and the basic proteins on the right of the gel image and descending molecular weights ranging from ~80 kDa to ~11 kDa. Varying protein spot abundances were the predominant difference between groups. Variations in individual gel images included minor deviations in pI and MW coordinates for assigned spots that were then aligned with 5 seed spots within the image analysis program.

3.3. Partial Least Squares - Discriminant Analysis

Iterative PLS-DA models were generated encompassing spot abundances of all proteins not determined to be noise with sequential removal of VIP-ranked protein spots contributing to the separation of groups and re-plotting of group separation until the loss of separation of groups was evident. Sixty-two protein spots (VIP≥1.5) were found to contribute to the separation in proteome profiles between the Sham and CSE groups. As shown in Figure 3A, when the abundances of all protein spots was included (noise excluded) the first latent factor accounted for 84% of the variance between the Sham and CSE groups and the second latent factor accounted for an additional 14% of the variance. As shown in Figure 3B, the combined descriptor representing individual protein spot abundances that comprise the proteome profiles of the Sham and CSE groups are distinct. The separation between the groups is depicted by graphing latent factors 1, 2 and 3.

3.4. Proteins Impacted by CSE

In Figure 4, a 2D-SDS-PAGE protein spot map is shown with numbers labeling the 62 protein spots identified as describing the separation between the Sham and CSE groups based on VIP>1.75 rankings as determined by Partial Least Squares-Discriminant Analysis. All proteins with p≤0.10 are also labeled in the figure as well as several protein spots used as markers that were not designated as altered in the kidney several months after withdrawal of CSE. For several spots (n=15), more than one protein was identified indicating that a mixture of proteins with similar isoelectric focusing point and molecular weight were present within the spot. Proteins that represent the predominant contribution to the spot intensity (as determined by a minimum of 200% of the MOWSE score of the next ranked protein identified) were included in the putative identification of nodes of interest within the networks impacted by developmental CSE see Tables 1 and 2). Of the 15 spots composed of multiple proteins (the intensity of 6 spots decreased, and that of 9 spots increased), a dominant protein attributed to the spot could be identified and was included in the Ingenuity® Pathway Analysis. The spots with multiple proteins present, but in which a dominant protein could be identified include: **Spots 18, 23, 28, 38, 48, 66**. The analysis did not include proteins from **Spot 30** (and similar spots) since the relative MOWSE scores for identification of the multiple proteins within the spot were similar and therefore a single likely candidate for alteration in abundance could not be identified. In **Spot 18**, both proteins identified were aldehyde dehydrogenase family members and thus it was included in the analysis.

Dominant or single proteins with altered abundance in kidneys of CSE mice were grouped by membership in metabolic networks via IPA analysis. As shown in Figure 5, a majority of proteins with altered abundance in the kidney of 6 month old mice that underwent prior

developmental CSE belonged to the nucleic acid metabolism, small molecular biochemistry, and carbohydrate metabolism pathways. Key nodes which may be affected in the adult kidney by developmental CSE include: HNF4α (Hepatocyte nuclear factor 4α) and Insulin. Each of these nodes plays a critical role in regulating glucose utilization.

The kidney proteins listed in Table 1 are decreased in abundance in 6 month old offspring that underwent prior developmental CSE (GD1-PD21). Proteins that are part of the *small molecule biochemistry network* remain decreased in abundance approximately 5 months after the discontinuation of the smoke exposure. Calreticulin, aldolase B, glyceraldehyde-3-phosphate dehydrogenase, and enoyl coenzyme A hydratase 1 were found to be decreased in abundance in our prior study of the kidney proteome at the time of cessation of developmental CSE and also were found, in the present study, to be decreased in abundance in the previously developmentally exposed kidney at maturity. Two enzymes linked to the *nucleic acid metabolism network* that were identified in our prior study of the kidney proteome (at the cessation of exposure) also remained decreased in abundance at maturity: aldolase B and glyceraldehyde-3-phosphate dehydrogenase. These proteins, however, retain redundant membership in multiple metabolic networks.

As listed in Table 2, several proteins that are members of the *lipid metabolism, small molecule and carbohydrate metabolism pathways* were increased in abundance in kidneys of 6 month old offspring (~5 months after cessation of CSE). Lambda crystallin, ATP synthase, H+ transporting, mitochondrial F1 complex, alpha subunit, aldehyde dehydrogenase family, subfamily A1, acetyl-Coenzyme A acetyltransferase 1, glutamate oxaloacetate transaminase 2, sorbitol dehydrogenase, ketohexokinase (also called fructokinase) were found in protein spots with increased abundance. Unaltered proteins that were identified in reference spots (checks of molecular weight and prior study comparison) are listed in Table 3.

3.5. Carbohydrate Metabolism Impacted by CSE

The top six canonical pathways impacted at 6 months of age in offspring exposed throughout development (GD1-PD21) to cigarette smoke are carbohydrate metabolic pathways which share common members (Figure 6). The abundance of four proteins belonging to the *Gluconeogenesis* pathway included aldolase B (**Spot 43**, decreased 45%), fructose-bisphosphate aldolase B (**Spot 42**, decreased 46%), glyceraldehyde-3-phosphate dehydrogenase (**Spots 46** and **47**, each decreased 40%), and malate dehydrogenase (**Spot 44**, increased 73%) were altered in abundance at 6 months of age following developmental cigarette smoke exposure. The Glycolysis pathway shared a decrease in abundance of three of these proteins: aldolase B, fructose-bis-phosphatase, and glyceraldehyde-3-phosphate dehydrogenase. The *Sucrose Degradation V* pathway included both aldolase B (**Spot 42**, decreased 46%) as well as ketohexokinase (**Spot 54**, increased 12%). The *Maturity Onset Diabetes of Young signaling* pathway included aldolase B and glyceraldehydre-3-phosphate dehydrogenase with the gluconeogenesis/glycolysis pathways. The *Sorbitol Degradation I* pathway consisted of a single member, sorbitol dehydrogenase (**Spot 29**, increased 28%). A lack of clear information on directionality of suppression of glucose synthesis/catabolism created challenges in determining whether both pathways were equally suppressed.

Follow-up studies of the expression level of SIRT1, a metabolic activity regulator, and the key regulatory enzyme in gluconeogenesis, phosphoenolpyruvate carboxykinase, revealed a trend toward decreased expression of basal gluconeogenesis within the fed state (Figure 7A and 7B). When paired to the finding of reduced serum glucose levels in the parallel study on liver tissue-specific toxicity in these same animals [47], these findings likely indicate systemic aberrant responses to insulin signaling or possible hyperinsulinemia. Insulin expression and signaling were not assessed within the current study.

Amino acid degradation was increased in kidneys at age 6 months of offspring within the CSE group, Glutamate oxaloacetate transaminase 1 (**Spot 26**, increased 37%) and malate dehydrogenase 2 (**Spot 44**, increased 73%) were members of the Aspartate Degradation II pathway and are both mitochondrial proteins. Several other mitochondrial proteins were increased in abundance including ATP synthase 5A1 (**Spot 20**, increased 126%), ATP synthase, H+ transporting, beta unit (**Spot 37**, increased 24%), and the voltage dependent anion channel 1 (**Spot 48**, increased 80%) indicating that mitochondrial activity or number is likely increased in the CSE offspring at 6 months of age. This added respiratory function would necessitate increased capacity for oxidant scavenging and indeed this is evidenced by the increased abundance of glutamate-cysteine ligase (**Spot 55**, increased 20%, glutathione synthesis) paired with increased glutathione peroxidase (**Spot 63**, increased 17%) and peroxiredoxin (**Spot 63**) in the CSE offspring. The specific activity of glutathione-S-transferase and glutathione reductase was not impacted in the CSE offspring.

4. DISCUSSION

In utero cigarette smoke exposure results in low birth weight with proportionally smaller organ size [60-63]. In the kidney, developmental CSE alters the shape of the proximal and distal convoluted tubules, reduces the proximal tubule cuboidal epithelium thickness, and yields immature glomeruli in neonates [64, 65]. As previously demonstrated, 'active' CSE during pre- and post-natal development, including the entirety of kidney organogenesis, results in low birth weight that is coupled to decreased offspring weights throughout postnatal development, although the rate of growth is unaffected [44]. Proportional decreases in offspring weight, crown-rump length, brain wet weight, and kidney weight in CSE offspring were observed [41, 61, 66].

In the current study, developmental exposure to an 'active' cigarette smoking paradigm results in persistently smaller offspring at maturity without evidence of catch up growth or obesity when offspring were maintained on a standard diet containing 12% of fat [49]. The persistently smaller phenotype of exposed mice includes proportionally smaller kidney mass coupled to sustained alterations in kidney proteome profiles. Decrements in kidney weight, a pseudomarker for decreased nephron count, were coupled to persistently decreased abundance of calreticulin. Decreased levels of calreticulin may also impact nephron count as calcium signaling is essential for the conversion of the metanephric mesenchyme into the functional nephron epithelium. The impact of developmental CSE on nephron count and morphology may contribute to the development of high blood pressure [67] or high-fat diet induced obesity [32]. We suggest that renal hyperfiltration and glomerular disease associated with a high-fat diet induced obesity paradigm may be exacerbated by the present model

system of 'active' cigarette smoke exposure throughout early development since increased nephron count and kidney mass do not accompany visceral fat accumulation [68]. Rather, reduced nephron number and kidney mass prior to obesity may increase the susceptibility to obesity-induced renal disease [69]. We plan to test this hypothesis in future studies.

As in our prior report at the time of animal weaning, the impact of developmental CSE on the kidney proteome at the cessation of exposure, the abundance of antioxidant enzymes Cu/Zn superoxide dismutase and glutathione peroxidase remained decreased in the CSE kidneys at maturity. Coupled with the finding of increased abundance of glutathione peroxidase and glutamate-cysteine ligase modifier subunit, and a lack of impact on the glutathione dependent antioxidant enzymes activities (GST and GR; Figure 8), we interpret this outcome as indicative of alterations in post-translational modification of these enzymes that do not inhibit function but may act as predisposing effectors with a subsequent challenge such as high dietary fat intake.

Of particular note in this study are the decreased abundance of three metabolic enzymes (Glyceraldehyde-3-phosphate dehydrogenase, Aldolase B, Fructose-1, 6-bisphosphatase) from the gluconeogenesis pathway. Aldolase B and Glyceraldehyde-3-dehydrogenase are also part of the glycolytic pathway. The decrease in abundance of these enzymes in the kidney of mature offspring who were developmentally exposed to cigarette smoke, coupled to the approximate 20% reduction in serum glucose levels in these animals [47] and the trend toward a reduction in tissue-specific PEPCK expression, indicates a deficit in glucose availability that may contribute to the decrements in growth and weight that are evident from birth and continue to maturity. It also appears that galactose utilization to produce glucose may be stimulated in the kidney of mature offspring developmentally exposed to cigarette smoke since galactose kinase abundance was increased. In contrast, within the liver of CSE offspring at 6 months of age, inappropriately timed gluconeogenesis appears to be occurring. This disparate, inverse relationship between hepatic and renal gluconeogenesis in the fed state may indicate an increased attempt to elevate basal gluconeogenesis by the liver which is not matched within the kidney. Indeed both tissues exhibited suppressed SIRT1 activation in the fed state but a disparate response by the gluconeogenesis pathway that may indicate tissue-specific involvement of the AMPK signaling network.

In contrast, increased abundance of sorbitol dehydrogenase and ketohexokinase in the kidney of mature offspring who were exposed throughout development (GD1-PD21) to cigarette smoke indicate a possible increase in conversion of glucose to fructose via the sorbitol pathway (sorbitol dehydrogenase protein spot abundance increased) and subsequent metabolism to produce the gluconeogenic precursor glyceraldehyde 3-phosphate or alternatively to proceed on to production of the lipogenic substrate pyruvate. We found that the abundance of malate dehydrogenase 2 (mitochondrial form) was increased substantiating the likely increased activity of the lipogenic pathway. Triglyceride levels in serum were unaltered in the mature exposed offspring (data not shown).

In summary, the current study examined the proteome profiles of the intact kidney from mature offspring (aged 6 months) who were previously developmentally exposed to CSE from GD1-PD21. At the time of cessation of exposure to cigarette smoke (PD21), proteins

involved in calcium signaling, lipid metabolism, and small molecule metabolism were decreased in abundance in the kidney, and oxidant scavenging enzymes, small heat shock proteins and lambda crystallin were increased in abundance [46]. As described in the current study of offspring five months past the cessation of exposure to cigarette smoke carbohydrate and small molecule metabolism as well as calcium regulation are again altered. The impact of developmental CSE on epigenetic programming of kidney metabolic function is the subject of future studies.

Acknowledgments

Research described in this article was supported in part by PHS grants NIH P20 RR/DE-17702, NIH R21 DA027466, NIH P30 ES014443 and by the University of Louisville CREAM Center from NSF EPSCoR grant EPS-0447479 (MS).

References

1. Li XY, Rahman I, Donaldson K, MacNee W. Mechanisms of cigarette smoke induced increased airspace permeability. Thorax. 1996; 51:465–71. [PubMed: 8711672]
2. Sisman AR, Bulbul M, Coker C, Onvural B. Cadmium exposure in tobacco workers: possible renal effects. J Trace Elem Med Biol. 2003; 17:51–5.
3. Kyerematen GA, Vesell ES. Metabolism of nicotine. Drug Metab Rev. 1991; 23:3–41. [PubMed: 1868776]
4. Shah PK, Helfant RH. Smoking and coronary artery disease. Chest. 1988; 94:449–52. [PubMed: 3409719]
5. Marcilla A, Martinez I, Berenguer D, Gomez-Siurana A, Beltran MI. Comparative study of the main characteristics and composition of the mainstream smoke of ten cigarette brands sold in Spain. Food Chem Toxicol. 2012; 50:1317–33. [PubMed: 22342527]
6. Shin HJ, Sohn HO, Han JH, Park CH, Lee HS, Lee DW, et al. Effect of cigarette filters on the chemical composition and in vitro biological activity of cigarette mainstream smoke. Food Chem Toxicol. 2009; 47:192–7. [PubMed: 19027817]
7. Rodgman A, Smith CJ, Perfetti TA. The composition of cigarette smoke: a retrospective, with emphasis on polycyclic components. Hum Exp Toxicol. 2000; 19:573–95. [PubMed: 11211997]
8. Bock FG, Swain AP, Stedman RL. Composition studies on tobacco. XLIV. Tumor-promoting activity of subfractions of the weak acid fraction of cigarette smoke condensate. J Natl Cancer Inst. 1971; 47:429–36. [PubMed: 5559243]
9. Bock FG, Swain AP, Stedman RL. Composition studies on tobacco. XLI. Carcinogenesis assay of subfractions of the neutral fraction of cigarette smoke condensate. J Natl Cancer Inst. 1970; 44:1305–10. [PubMed: 11515451]
10. Lindsey AJ. The composition of cigarette smoke: studies on stubs and tips. Br J Cancer. 1959; 13:195–9. [PubMed: 14417209]
11. Righetti M, Sessa A. Cigarette smoking and kidney involvement. J Nephrol. 2001; 14:3–6. [PubMed: 11281341]
12. Teshima K, Imamura H, Uchida K, Miyamoto N, Masuda Y, Kobata D. Cigarette smoking, blood pressure and serum lipids in Japanese men aged 20–39 years. J Physiol Anthropol Appl Human Sci. 2001; 20:43–5.
13. Will JC, Galuska DA, Ford ES, Mokdad A, Calle EE. Cigarette smoking and diabetes mellitus: evidence of a positive association from a large prospective cohort study. Int J Epidemiol. 2001; 30:540–6. [PubMed: 11416080]
14. Winkelmann BR, Boehm BO, Nauck M, Kleist P, Marz W, Verho NK, et al. Cigarette smoking is independently associated with markers of endothelial dysfunction and hyperinsulinaemia in nondiabetic individuals with coronary artery disease. Curr Med Res Opin. 2001; 17:132–41. [PubMed: 11759183]

15. Zevin S, Saunders S, Gourlay SG, Jacob P, Benowitz NL. Cardiovascular effects of carbon monoxide and cigarette smoking. J Am Coll Cardiol. 2001; 38:1633–8. [PubMed: 11704374]
16. Charlton A. Changing patterns of cigarette smoking among teenagers and young adults. Paediatr Respir Rev. 2001; 2:214–21. [PubMed: 12052322]
17. Christiansen AL, Malmstadt J, Rumm P, Eisenberg T, Ahrens D, Remington P. Trends in self-reported cigarette smoking, Wisconsin, 1984–1999. WMJ. 2001; 100:24–8.
18. Moffat BM, Johnson JL. Through the haze of cigarettes: teenage girls' stories about cigarette addiction. Qual Health Res. 2001; 11:668–81. [PubMed: 11554194]
19. Molarius A, Parsons RW, Dobson AJ, Evans A, Fortmann SP, Jamrozik K, et al. Trends in cigarette smoking in 36 populations from the early 1980s to the mid-1990s: findings from the WHO MONICA Project. Am J Public Health. 2001; 91:206–12. [PubMed: 11211628]
20. Watson R. MEPs back tougher health warnings on cigarette packets. BMJ. 2001; 322:7.
21. CDC. Cigarette smoking in 99 metropolitan areas--United States, 2000. MMWR Morb Mortal Wkly Rep. 2001; 50:1107–13. [PubMed: 11794621]
22. CDC. Cigarette smoking among adults--United States, 1999. MMWR Morb Mortal Wkly Rep. 2001; 50:869–73. [PubMed: 11666113]
23. Lewis PC, Harrell JS, Bradley C, Deng S. Cigarette use in adolescents: the Cardiovascular Health in Children and Youth Study. Res Nurs Health. 2001; 24:27–37. [PubMed: 11260583]
24. Boutwell BB, Beaver KM, Gibson CL, Ward JT. Prenatal exposure to cigarette smoke and childhood externalizing behavioral problems: a propensity score matching approach. Int J Environ Health Res. 2011; 21:248–59. [PubMed: 21598153]
25. Koshy G, Delpisheh A, Brabin BJ. Dose response association of pregnancy cigarette smoke exposure, childhood stature, overweight and obesity. Eur J Public Health. 2011; 21:286–91. [PubMed: 21126981]
26. Stack AG, Murthy BV. Cigarette use and cardiovascular risk in chronic kidney disease: an unappreciated modifiable lifestyle risk factor. Semin Dial. 2010; 23:298–305. [PubMed: 20636923]
27. Gambaro G, Bax G, Fusaro M, Normanno M, Manani SM, Zanella M, et al. Cigarette smoking is a risk factor for nephropathy and its progression in type 2 diabetes mellitus. Diabetes Nutr Metab. 2001; 14:337–42. [PubMed: 11853366]
28. Gulliford MC. Low rates of detection and treatment of hypertension among current cigarette smokers. J Hum Hypertens. 2001; 15:771–3. [PubMed: 11687920]
29. Imamura H, Miyamoto N, Uchida K, Teshima K, Masuda Y, Kobata D. Cigarette smoking, blood pressure and serum lipids and lipoproteins in middle-aged women. J Physiol Anthropol Appl Human Sci. 2001; 20:1–6.
30. von Holt K, Lebrun S, Stinn W, Conroy L, Wallerath T, Schleef R. Progression of atherosclerosis in the Apo E-/- model: 12-month exposure to cigarette mainstream smoke combined with high-cholesterol/fat diet. Atherosclerosis. 2009; 205:135–43. [PubMed: 19144336]
31. Chen H, Hansen MJ, Jones JE, Vlahos R, Anderson GP, Morris MJ. Detrimental metabolic effects of combining long-term cigarette smoke exposure and high-fat diet in mice. Am J Physiol Endocrinol Metab. 2007; 293:E1564–71. [PubMed: 17940214]
32. Ng SP, Conklin DJ, Bhatnagar A, Bolanowski DD, Lyon J, Zelikoff JT. Prenatal exposure to cigarette smoke induces diet- and sex-dependent dyslipidemia and weight gain in adult murine offspring. Environ Health Perspect. 2009; 117:1042–8. [PubMed: 19654910]
33. Chen H, Iglesias MA, Caruso V, Morris MJ. Maternal cigarette smoke exposure contributes to glucose intolerance and decreased brain insulin action in mice offspring independent of maternal diet. PLoS One. 2011; 6:e27260. [PubMed: 22076142]
34. Zarzecki M, Adamczak M, Wystrychowski A, Gross ML, Ritz E, Wiecek A. Exposure of Pregnant Rats to Cigarette-Smoke Condensate Causes Glomerular Abnormalities in Offspring. Kidney Blood Press Res. 2012; 36:162–71. [PubMed: 23095255]
35. Younoszai MK, Peloso J, Haworth JC. Fetal growth retardation in rats exposed to cigarette smoke during pregnancy. Am J Obstet Gynecol. 1969; 104:1207–13. [PubMed: 5799624]
36. Abitbol CL, Ingelfinger JR. Nephron mass and cardiovascular and renal disease risks. Semin Nephrol. 2009; 29:445–54. [PubMed: 19615565]

37. Dotsch J, Plank C, Amann K, Ingelfinger J. The implications of fetal programming of glomerular number and renal function. J Mol Med (Berl). 2009; 87:841–8. [PubMed: 19652918]
38. Tsuboi N, Utsunomiya Y, Hosoya T. Obesity-related glomerulopathy and the nephron complement. Nephrol Dial Transplant. 2013; 28(Suppl 4):iv108–13. [PubMed: 23868145]
39. Tsuboi N, Koike K, Hirano K, Utsunomiya Y, Kawamura T, Hosoya T. Clinical features and long-term renal outcomes of Japanese patients with obesity-related glomerulopathy. Clin Exp Nephrol. 2013; 17:379–85. [PubMed: 23135866]
40. Toledo-Rodriguez M, Loyse N, Bourdon C, Arab S, Pausova Z. Effect of prenatal exposure to nicotine on kidney glomerular mass and AT1R expression in genetically diverse strains of rats. Toxicol Lett. 2012; 213:228–34. [PubMed: 22728133]
41. Jagadapillai R, Chen J, Canales L, Birtles T, Pisano MM, Neal RE. Developmental cigarette smoke exposure: kidney proteome profile alterations in low birth weight pups. Toxicology. 2012; 299:80–9. [PubMed: 22595367]
42. Rueff-Barroso CR, Trajano ET, Alves JN, Paiva RO, Lanzetti M, Pires KM, et al. Organ-related cigarette smoke-induced oxidative stress is strain-dependent. Med Sci Monit. 2010; 16:BR218–26. [PubMed: 20581770]
43. Mao C, Wu J, Xiao D, Lv J, Ding Y, Xu Z, et al. The effect of fetal and neonatal nicotine exposure on renal development of AT(1) and AT(2) receptors. Reprod Toxicol. 2009; 27:149–54. [PubMed: 19429393]
44. Canales L, Chen J, Kelty E, Musah S, Webb C, Pisano MM, et al. Developmental cigarette smoke exposure: liver proteome profile alterations in low birth weight pups. Toxicology. 2012; 300:1–11. [PubMed: 22609517]
45. Neal RE, Chen J, Jagadapillai R, Jang H, Abomoelak B, Brock G, et al. Developmental cigarette smoke exposure: hippocampus proteome and metabolome profiles in low birth weight pups. Toxicology. 2014; 317:40–9. [PubMed: 24486158]
46. Neal R, Jagadapillai R, Chen J, Stocke K, Gambrell C, Greene RM, Pisano MM. Developmental Cigarette Smoke Exposure II: Kidney Proteome Profile Alterations in Adult Offspring. Reprod Toxicol. 2016 X:X.
47. Neal RE, Chen J, Stocke K, Webb C, Gambrell C, Greene RM, Pisano MM. Developmental Cigarette Smoke Exposure II: Hepatic Proteome Profiles in Adult Offspring. Reprod Toxicol. 2016 x:x.
48. Neal RE, Jagadapillai R, Chen J, Stocke K, Webb C, Greene RM, Pisano MM. Developmental cigarette smoke exposure II: Hippocampus proteome and metabolome profiles in adult offspring. Reprod Toxicol. 2016 x:x.
49. Amos-Kroohs RM, Williams MT, Braun AA, Graham DL, Webb CL, Birtles TS, et al. Neurobehavioral phenotype of C57BL/6J mice prenatally and neonatally exposed to cigarette smoke. Neurotoxicol Teratol. 2013; 35:34–45. [PubMed: 23314114]
50. CDC. Incidence of initiation of cigarette smoking--United States, 1965-1996. MMWR Morb Mortal Wkly Rep. 1998; 47:837–40. [PubMed: 9780240]
51. Husten CG, Chrismon JH, Reddy MN. Trends and effects of cigarette smoking among girls and women in the United States, 1965-1993. J Am Med Womens Assoc. 1996; 51:11–8. [PubMed: 8868541]
52. Nelson DE, Giovino GA, Shopland DR, Mowery PD, Mills SL, Eriksen MP. Trends in cigarette smoking among US adolescents, 1974 through 1991. Am J Public Health. 1995; 85:34–40. [PubMed: 7832259]
53. CDC. Comparison of the cigarette brand preferences of adult and teenaged smokers--United States, 1989, and 10 U.S. communities, 1988 and 1990. MMWR Morb Mortal Wkly Rep. 1992; 41:169–73. 79–81. [PubMed: 1538687]
54. Teague SV, Pinkerton KE, Goldsmith M, Gebremichael A, Chang S, Jenkins RA, Moneyhun JH. Sidestream cigarette smoke generation and exposure system for environmental tobacco smoke studies. Inhalation Toxicology. 1994; 6:79–93.
55. Pappin DJ, Hojrup P, Bleasby AJ. Rapid identification of proteins by peptide-mass fingerprinting. Curr Biol. 1993; 3:327–32. [PubMed: 15335725]

56. Gershoni JM. Protein blotting: a manual. Methods Biochem Anal. 1988; 33:1–58. [PubMed: 2451778]
57. Boyland E, Chasseaud LF. Glutathione S-aralkyltransferase. Biochem J. 1969; 115:985–91. [PubMed: 5360727]
58. Jakoby WB. The glutathione S-transferases: a group of multifunctional detoxification proteins. Adv Enzymol Relat Areas Mol Biol. 1978; 46:383–414. [PubMed: 345769]
59. Staal GE, Visser J, Veeger C. Purification and properties of glutathione reductase of human erythrocytes. Biochim Biophys Acta. 1969; 185:39–48. [PubMed: 5796111]
60. Horn KH, Esposito ER, Greene RM, Pisano MM. The effect of cigarette smoke exposure on developing folate binding protein-2 null mice. Reprod Toxicol. 2008; 26:203–9. [PubMed: 18992323]
61. Esposito ER, Horn KH, Greene RM, Pisano MM. An animal model of cigarette smoke-induced in utero growth retardation. Toxicology. 2008; 246:193–202. [PubMed: 18316152]
62. Prabhu N, Smith N, Campbell D, Craig LC, Seaton A, Helms PJ, et al. First trimester maternal tobacco smoking habits and fetal growth. Thorax. 2010; 65:235–40. [PubMed: 20335293]
63. Cliver SP, Goldenberg RL, Cutter GR, Hoffman HJ, Davis RO, Nelson KG. The effect of cigarette smoking on neonatal anthropometric measurements. Obstet Gynecol. 1995; 85:625–30. [PubMed: 7898845]
64. Czekaj P, Palasz A, Lebda-Wyborny T, Nowaczyk-Dura G, Karczewska W, Florek E, et al. Morphological changes in lungs, placenta, liver and kidneys of pregnant rats exposed to cigarette smoke. Int Arch Occup Environ Health. 2002; 75(Suppl):S27–35. [PubMed: 12397408]
65. Nelson E, Goubet-Wiemers C, Guo Y, Jodscheit K. Maternal passive smoking during pregnancy and foetal developmental toxicity. Part 2: histological changes. Hum Exp Toxicol. 1999; 18:257–64. [PubMed: 10333312]
66. Neal RE, Chen J, Jagadapillai R, Jang HJ, Abomoelak B, Brock G, et al. Developmental Cigarette Smoke Exposure: Hippocampus Proteome and Metabolome Profiles in Low Birth Weight Pups. Toxicology. 2014 In Press.
67. Zarzecki M, Adamczak M, Wystrychowski A, Gross ML, Ritz E, Wiecek A. Exposure of pregnant rats to cigarette-smoke condensate causes glomerular abnormalities in offspring. Kidney Blood Press Res. 2012; 36:162–71. [PubMed: 23095255]
68. Praga M. Synergy of low nephron number and obesity: a new focus on hyperfiltration nephropathy. Nephrol Dial Transplant. 2005; 20:2594–7. [PubMed: 16223782]
69. Gurusinghe S, Brown RD, Cai X, Samuel CS, Ricardo SD, Thomas MC, et al. Does a nephron deficit exacerbate the renal and cardiovascular effects of obesity? PLoS One. 2013; 8:e73095. [PubMed: 24019901]

Highlights

- Developmental CSE induces impairment of carbohydrate metabolic pathway protein expression.
- Oxidant scavenging pathways are impaired in adults by developmental CSE.
- Decreased protein abundances within the nucleic acid metabolic pathways evident in mature CSE offspring

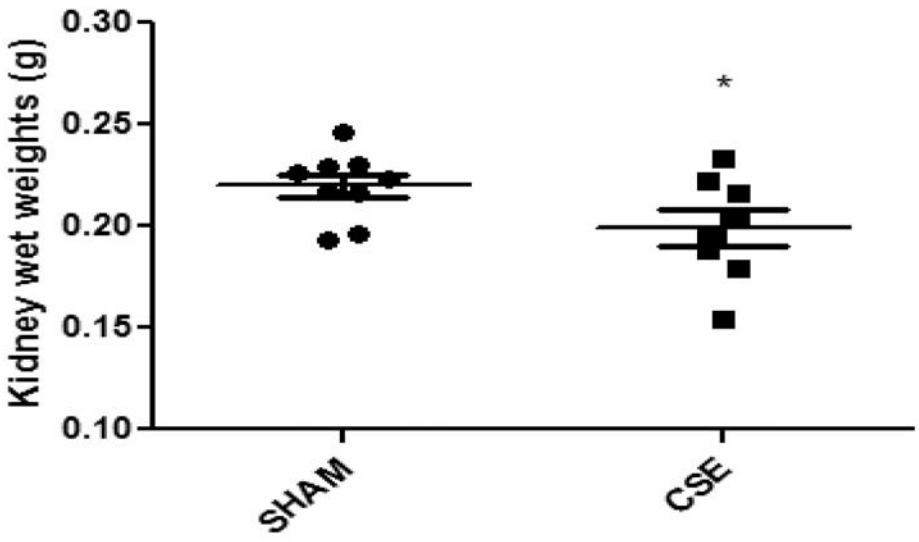

Figure 1. Kidney tissue wet weights were reduced at 6 months of age following developmental exposure to cigarette smoke (GD1-PD21)

Kidneys from offspring exposed to either filtered air (SHAM, n=9) or a protocol of "active" cigarette smoking (CSE, n=8) during development were weighed following animal euthanization at 6 months of age (*$p<0.05$). Long horizontal lines indicate mean weight, with the standard deviation represented by the shorter horizontal bars.

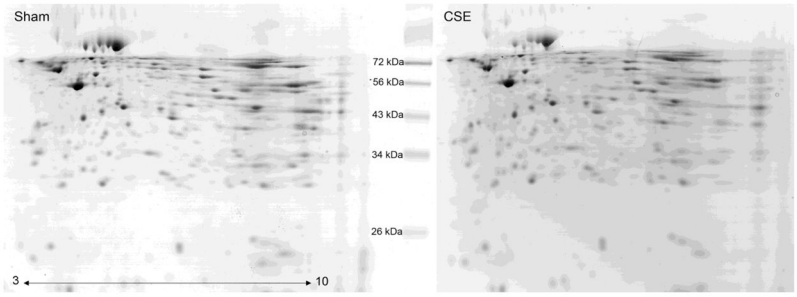

Figure 2. Side-by-side comparison of protein spot patterns of kidney from the Sham and developmental CSE groups

A side-by-side comparison of kidney protein spot separation based on isoelectric focusing point (horizontal) and molecular weight (vertical) in the two experimental groups (Sham-left; CSE-right). The gels are similar with regard to the number of spots without the appearance or loss of spots between groups.

Figure 3A

Latent Factor	Y Variance	Cumulative Y Variance (R squared)
1	0.84	0.84
2	0.14	0.98

Figure 3B

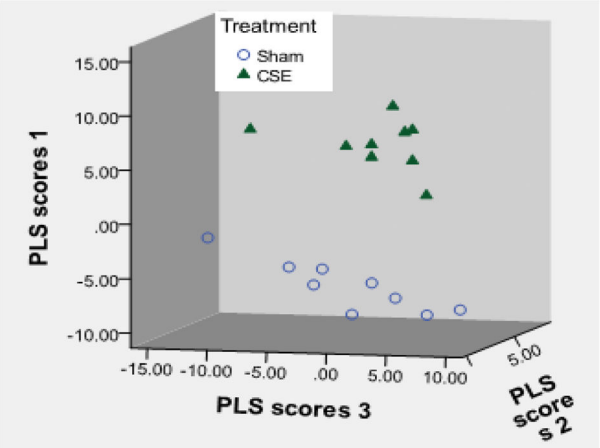

Figure 3.

Figure 3A: Variable importance in projection. Protein spots present on gels from the Sham and developmental CSE groups were analyzed by PLS-DA (n=9 per group, biological replicates). Description of the separation of groups by latent factors found that 99% of the variance between groups could be described by two latent factors.

Figure 3B: Plotting latent factors from the PLS-DA model shows differences in the kidney protein spot patterns of the Sham and developmental CSE groups at 6 months of age. All protein spots (excluding noise) were included in the calculation of VIP rankings and the graphing of the separation of groups by latent factors.

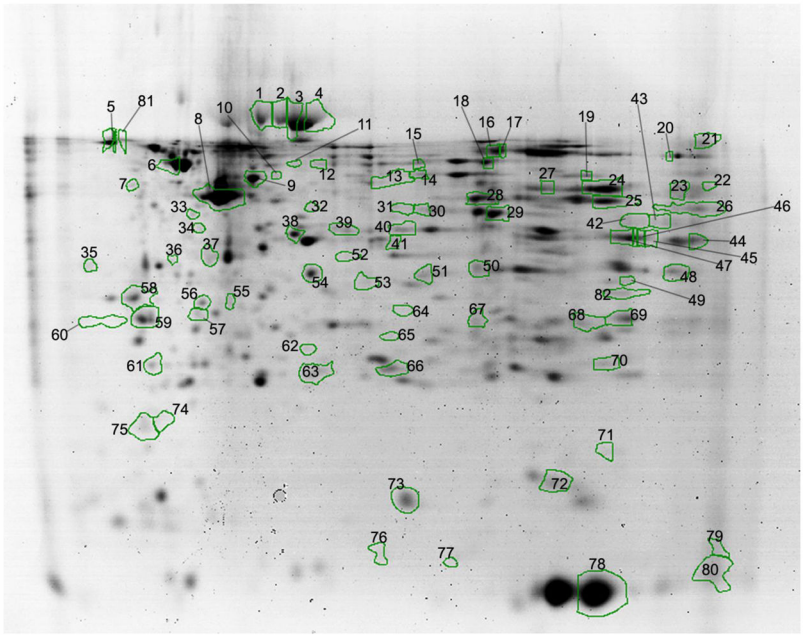

Figure 4. Kidney proteome profiles of 6 month old offspring previously developmentally exposed to cigarette smoke

The proteins with altered abundance that contributed to the separation of the groups within the PLS-DA model and possessed the highest VIP values (≥1.75) are numbered (as well as a limited selection of unaltered proteins) Refer to Tables 1–3, for a listing of proteins identified in each spot.

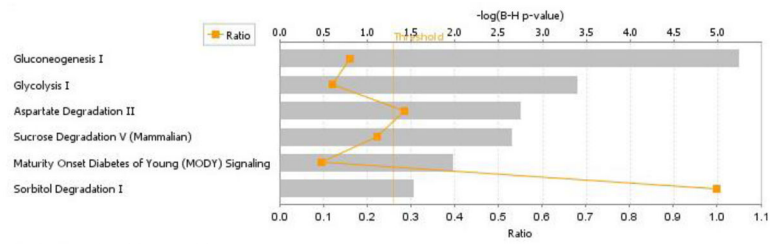

Figure 5. The top six ranked protein interaction networks and pathways impacted within the liver of adult offspring who were previously developmentally exposed to cigarette smoke

The distance from the threshold value (vertical, orange line) depicts the intensity of change between Sham exposure and CSE groups.

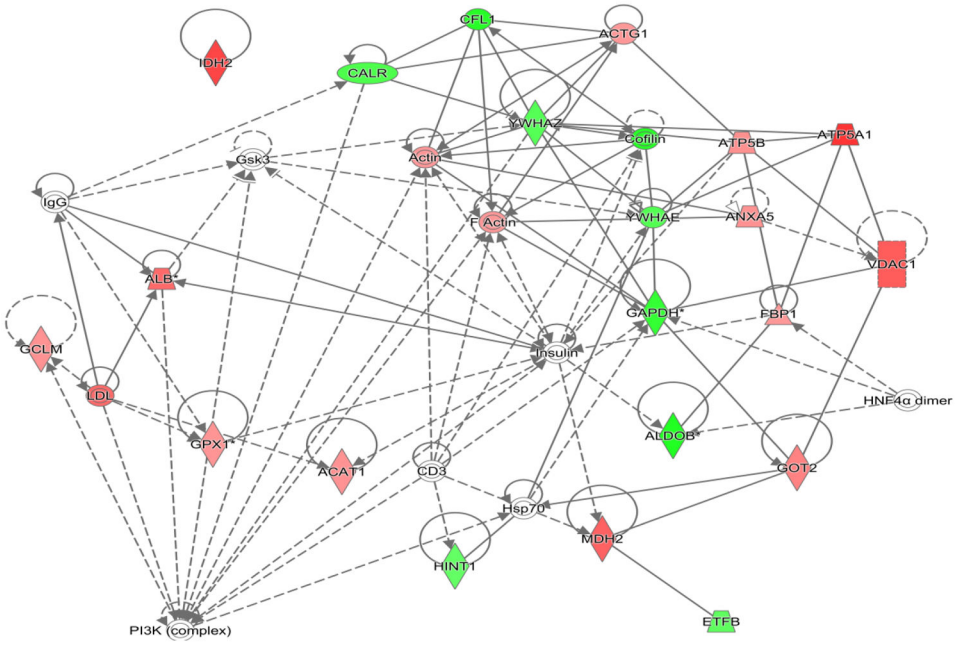

Figure 6. Nucleic acid metabolism, small molecule biochemistry, and carbohydrate metabolism pathways in the adult kidney affected by developmental CSE

Kidney proteins identified as contributing to the separation of groups (Sham exposed and CSE) are shadowed and connected to the network by arrows denoting directionality of interaction. Solid lines indicated a direct interaction while dotted lines indicate an indirect interaction. Geometric shapes identify classes of proteins: phosphatases (triangle), kinases (inverted triangle), enzymes (vertical diamond), transcription regulators (horizontal ellipse), transporters (trapezoid), and other important molecules (circles). Red indicates increased abundance while green indicates decreased abundance in the CSE group. Abbreviations are defined in Tables 1 and 2.

Figure 7A

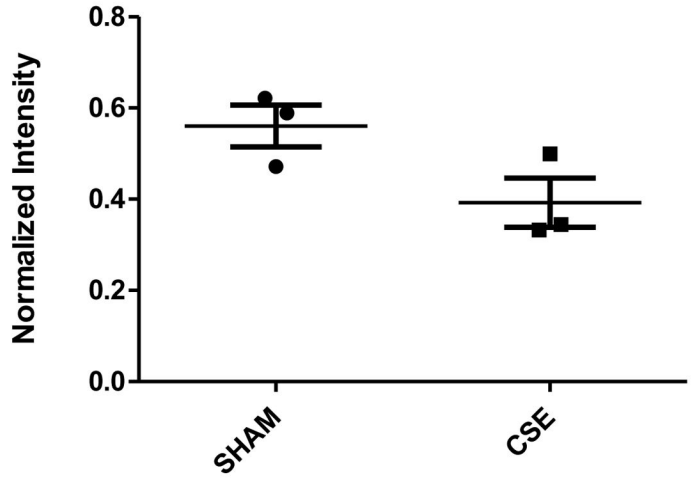

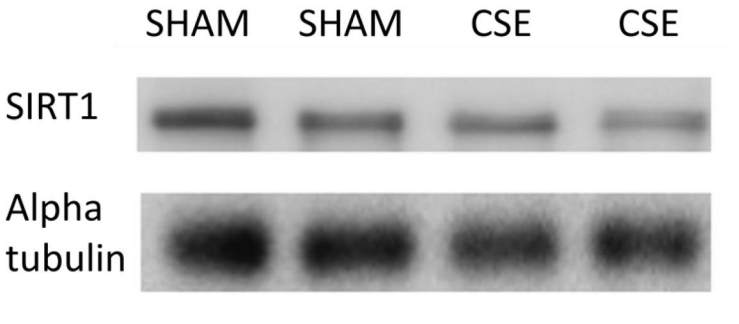

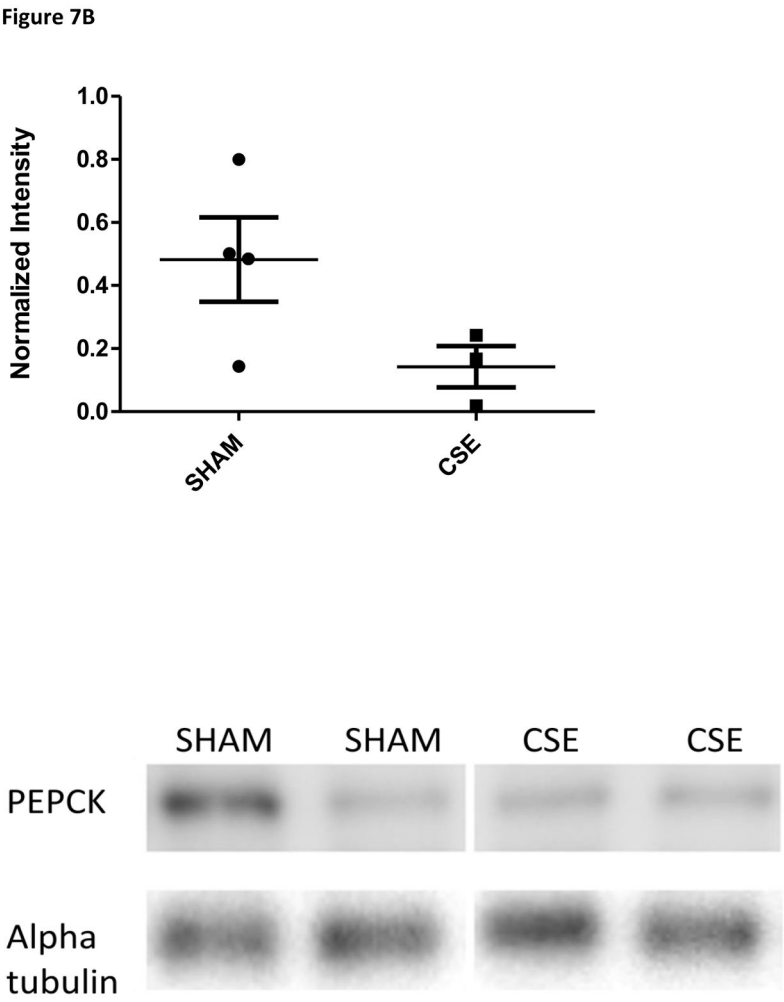

Figure 7.

Figure 7A: Western blot analysis of SIRT1 expression in whole kidney homogenates from 6 month old offspring previously exposed on GD1-PD21 to cigarette smoke. Kidney homogenates from CSE offspring at age 6 months exhibited a decrease of approximately 30% in expression of the metabolic regulatory protein SIRT1 when compared to Sham exposed (*$p<0.05$; n=3 per group). Long horizontal lines indicate mean signal intensity, with the standard deviation represented by the shorter horizontal bars.

Figure 7B: Western blot analysis of PEPCK expression in whole kidney homogenates from 6 month old offspring previously exposed GD1-PD21 to cigarette smoke. Kidney homogenates from CSE offspring at age 6 months exhibited an increase of approximately 70% in PEPCK expression in the fed state when compared to Sham exposed (*$p<0.05$; n=4 per group). Long horizontal lines indicate mean signal intensity, with the standard deviation represented by the shorter horizontal bars.

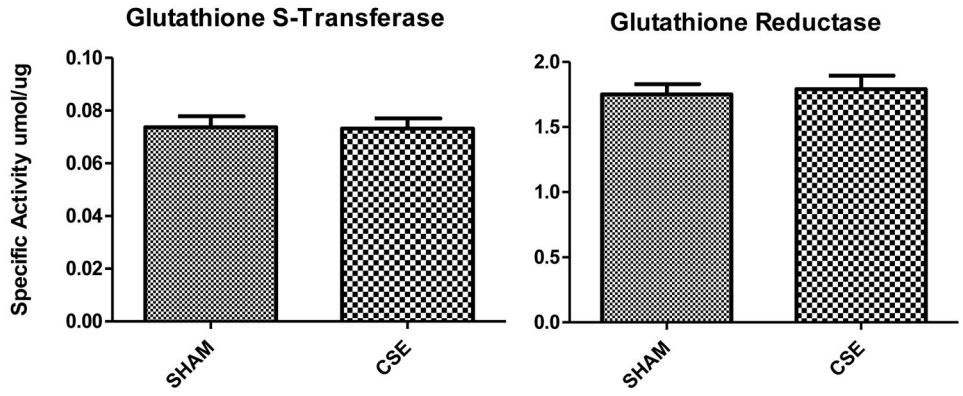

Figure 8. Antioxidant enzymatic activity in kidney of Sham and developmental CSE offspring at age 6 months

Antioxidant enzyme specific activity was *not* compromised in the kidney of CSE offspring (n=4 per group).

Table 1

Identification of proteins from spots with decreased abundance that contributed to the separation of kidney proteome profiles of mature offspring previously exposed to cigarette smoke throughout development (GD1-PD21) [PLS-DA model, VIP values (≥1.75)]

VIP (Variable Importance in Projection); GI Number (NCBI protein sequence *GenInfo Identifier*).

Spot	GI Number	Abbreviation[1]	Name	VIP	Percent Change
1	435838		mortalin mot-1=hsp70 homolog cytosolic form	1.78	21
2	163310765		albumin	1.80	27
3	163310765		albumin	1.48	19
13			No ID	1.45	38
15			No ID	1.42	15
30	9789985 13195624		isovaleryl coenzyme A dehydrogenase NADH dehydrogenase (ubiquinone) 1 alpha subcomplex 10	1.99	25
40			No ID	1.67	20
42	15723268	ALDOB	fructose-bisphosphate aldolase B	1.99	46
43	21450291 22267442	ALDOB	aldolase B, fructose-bisphosphate ubiquinol cytochrome c reductase core protein 2	2.11	45
45	62653546		PREDICTED: similar to glyceraldehyde-3- phosphate dehydrogenase	1.73	25
46	6679937	GAPDH	glyceraldehyde-3-phosphate dehydrogenase	2.09	40
47	6679937	GAPDH	glyceraldehyde-3-phosphate dehydrogenase	2.31	40
49			No ID	1.60	47
51	7949037 63100260 6755965 17921976		enoyl coenzyme A hydratase 1, peroxisomal mercaptopyruvate sulfurtransferase voltage-dependent anion channel 2 3-hydroxyanthranilate 3,4-dioxygenase	1.58	16
53			No ID	1.56	19
58	13928824 5902663	YWHAE	tyrosine 3-monooxygenase/tryptophan 5- monooxygenase activation protein elongation factor 1-beta homolog	1.46	30
59	6756041	YWHAZ	tyrosine 3-monooxygenase/tryptophan 5- monooxygenase activation protein, zeta polypeptide	2.22	29
64			No ID	1.98	20
65			No ID	1.59	19
66	84871986 55741460		glutathione peroxidase 1 parkinson disease protein 7	1.78	11

Spot	GI Number	Abbreviation[1]	Name	VIP	Percent Change
69	38142460	ETFB	electron transferring flavoprotein, beta polypeptide	2.00	25
71	6680924	Cofilin/CFL1	cofilin 1, non-muscle	2.00	44
73	226471		Cu/Zn superoxide dismutase	1.96	10
74	11935049 154937382 127527		cytokeratin 2 myosin, light chain 9, regulatory major urinary protein 2	1.54	22
77	33468857	HINT1	histidine triad nucleotide binding protein 1	1.77	22
79	229301		hemoglobin beta	1.82	37
81	6680836	CALR	calreticulin	1.72	32

[1]Denotes abbreviation used in Figure 6.

Reprod Toxicol. Author manuscript; available in PMC 2017 October 01.

Table 2

Identification of proteins from spots with increased abundance that contributed to the separation of kidney proteome profiles of mature offspring previously exposed to cigarette smoke throughout development (GD1-PD21) [PLS-DA model, VIP values (≥1.75)]

VIP (Variable Importance in Projection); GI Number (NCBI protein sequence *GenInfo Identifier*). Corresponds to Figure 1.

Spot	GI Number	Abbreviation [1]	Name	VIP	Percent Change
4	163310765	ALB*	albumin	1.96	64
5			No ID	2.14	101
6			No ID	1.65	13
8	6425087	ACTG1	gamma actin-like protein	1.89	12
9	14548301		cytochrome b-c1 complex subunit 1, mitochondrial	1.43	9
10			No ID	1.72	19
16			No ID	1.46	31
17	19527258		aldehyde dehydrogenase family 6, subfamily A1	1.8	36
18	78099319 6753036		aldehyde dehydrogenase family 9 member A1 mitochondrial aldehyde dehydrogenase 2	1.33	31
20	148677501	ATP5A1	ATP synthase, H+ transporting, mitochondrial F1 complex, alpha subunit, isoform 1, isoform CRA_e	1.58	126
21			No ID	1.78	65
22			No ID	1.66	173
23	12003362 22267442 6996911	IDH2	NADP+-specific isocitrate dehydrogenase ubiquinol cytochrome c reductase core protein 2 argininosuccinate synthetase 1	1.66	105
25	21450129	ACAT1	acetyl-Coenzyme A acetyltransferase 1 precursor	1.51	19
26	6754036	GOT2	glutamate oxaloacetate transaminase 2, mitochondrial	1.48	37
28	9789985 21450129		isovaleryl coenzyme A dehydrogenase acetyl-Coenzyme A acetyltransferase 1 precursor	1.87	18
29	22128627		sorbitol dehydrogenase	2.11	28
31			No ID	1.60	16
32			No ID	1.79	42
33	11132435		galactose kinase	1.41	20

Spot	GI Number	Abbreviation [1]	Name	VIP	Percent Change
34			No ID	1.57	20
35	31982300		hemoglobin, beta adult major chain	1.27	110
36	6753060 155369696	ANXA5	annexin A5 hypothetical protein LOC683313	1.51	19
37	31982632	ATP5B	aspartoacylase 3	1.75	24
	1374715		ATP synthase beta subunit		
38	19525729 11560131		crystallin, lambda 1 dimethylarginine dimethylaminohydrolase 1	1.51	10
39	9506589	FBP1	fructose-1,6-bisphosphatase 1	1.47	12
44	31982186 6679937	MDH2	malate dehydrogenase 2, NAD (mitochondrial) glyceraldehyde-3-phosphate dehydrogenase	1.61	73
48	6755963 13385680	VDAC1	voltage-dependent anion channel 1 2,4-dienoyl CoA reductase 1	2.14	80
54	31982229		ketohexokinase	1.44	12
55	6680019	GCLM	glutamate-cysteine ligase, modifier subunit	2.06	20
56	15617203		chloride intracellular channel 1	2.07	22
57	1374715	ATP5B	ATP synthase beta subunit	1.51	21
60			No ID	1.31	33
62			No ID	1.62	23
63	2673845 17389257 6754976	GPX1	glutathione peroxidase cytidine monophosphate (UMP-CMP) kinase 1 peroxiredoxin 1	1.68	17

[1] Denotes abbreviation used in Figure 6.

Reprod Toxicol. Author manuscript; available in PMC 2017 October 01.

Table 3

Identified proteins with no change in abundance and which did not contribute to the separation of kidney proteome profiles of mature offspring previously exposed to cigarette smoke during development (GD1-PD21)

VIP (Variable Importance in Projection); GI Number (NCBI protein sequence *GenInfo Identifier*).

Spot	GI Number	Name	VIP
7		No ID	0.08
27	6647554	isocitrate dehydrogenase [NADP] cytoplasmic	0.05
11		No ID	1.36
12		No ID	1.40
14	70794816	hypothetical protein LOC433182	1.33
19	21431774	fumarate hydratase, mitochondrial	1.44
24	6996911 202423	argininosuccinate synthetase 1 phosphoglycerate kinase	1.38
41		No ID	1.27
50	13097375	electron transferring flavoprotein, alpha polypeptide	1.40
52	387129	cytosolic malate dehydrogenase	1.35
61		No ID	1.78
67		No ID	1.20
68	29789289	mitochondrial short-chain enoyl-coenzyme A hydratase 1	1.47
70	10092608	glutathione S-transferase, pi 1	1.37
72		No ID	1.27
75	31542438	cytochrome b5 type B precursor	1.27
76	7305599	transthyretin	0.09
78	122441	hemoglobin subunit alpha	1.42
80	229301	hemoglobin beta	1.37
82	6680748	ATP synthase, H+ transporting, mitochondrial F1 complex, alpha subunit, isoform 1	1.31